International Journal of Adhesion & Adhesives 29 (2009) 633–638

Contents lists available at ScienceDirect

International Journal of Adhesion & Adhesives

journal homepage: www.elsevier.com/locate/ijadhadh

Study on the fatigue strength of AA 6082-T6 adhesive lap joints

A.M. Pereira [a,*], J.M. Ferreira [b], F.V. Antunes [b], P.J. Bártolo [a]

[a] CDRsp, Centre for Rapid and Sustainable Product Development, Polytechnic Institute of Leiria, Morro do Lena-Alto Vieiro, 2400-901 Leiria, Portugal
[b] CEMUC, Centre of Mechanical Engineering of University of Coimbra, Polo II da Univ. of Coimbra, Pinhal de Marrocos, 3030-788 Coimbra, Portugal

ARTICLE INFO

Available online 6 March 2009

Keywords:
Aluminium and alloys
Surface treatment
Finite element stress analysis
Fatigue

ABSTRACT

A research study on the fatigue behaviour of aluminium alloy adhesive lap joints was carried out to understand the effect of surface pre-treatment and adherends thickness on the fatigue strength of adhesive joints. The adherend material used for the experimental tests was an aluminium alloy 6082-T6 in the form of thin sheets, and the adhesive used was a high strength epoxy (Araldite 420 A/B). The surface preparation included an abrasive preparation (AP joints) and sodium dichromate–sulphuric acid etch (CSA joints).

A maximum fatigue strength was obtained for the CSA surface treatment with a 1.0 mm adherends' thickness. The fastest fatigue damage was related with a high surface roughness and a high stress perpendicular to adhesive surface, which helps to promote the adhesive failure. A numerical analysis was also performed to understand the effect of the adherends thickness on the stress level. Results showed an increase of the out-of-plane peak stresses with the increase of adherends thickness.

1. Introduction

Increasing restrictions are being imposed in terms of performance, pollution, safety and energy consumptions for the production of components and equipments, namely those of transportation vehicles, so there must be an effort to use new materials and processes to promote weight reduction. Improvements can be obtained with lighter materials like aluminium alloys, and better joining processes as adhesive bonding. Adhesive bonding is a cheap, fast and robust joining technique increasingly used in structural applications, such as car, aerospace, electronics and electric industries.

Adhesive bonding offers advantages relatively to other conventional joining processes, namely acoustic isolation, vibration attenuation, reduction of corrosion problems, and a more uniform stress distribution. Chang et al. [1], Ghosh and Vivek [2] and Santos et al. [3] conducted studies to characterize and compare the performance of resistance spot welding, adhesive bonding and weldbonding joining processes under static loading. In a recent work, Ferreira et al. [4] studied the stress field in adhesive joints of polypropylene/glass fibre laminates, using the finite element method.

In other works, Pereira et al. [5] studied the stress field in adhesive joints of aluminium alloys to improve the understanding of experimental results concerning the effect of geometric parameters, such as the adhesive thickness on the shear strength of single lap joints. The effect of other manufacture parameters was investigated, such as the surface pre-treatment and manufacturing pressure, allowing the optimization of the bonding technique.

The static behaviour of adhesive joints has been extensively studied [6–8]. However, its fatigue strength needs to be better understood. Fatigue behaviour needs a significant research improvement in order to understand the failure mechanisms and the influence of parameters like surface pre-treatment, adhesive thickness or adherends thickness. Rushforth et al. [9] studied the effect of surface pre-treatment and moisture on the fatigue performance of single lap adhesively bonded aluminium joints, showing the importance of pre-treatment in sustaining the fatigue performance of bonded single lap joints under humid conditions. Adams et al. [10] demonstrated that the tensile fatigue properties, at room temperature, were strongly affected by the surface preparation, even when the fatigue tests were conducted in dry air. Briskam and Smith [11] have studied shear lap joints and found that its fatigue life is also strongly influenced by the surface preparation. Underhill and Duquesnay [12] investigated the influence of silane pre-treatment on the fatigue life of epoxy-bonded single-lap shear joints under both dry and wet conditions. They concluded, for dry condition, that the fatigue life of unsilaned joints was reduced by about an order of magnitude compared to the silaned joints. Krenk et al. [13] studied the fatigue resistance behaviour of a single lap aluminium adhesive joint for an adhesive thickness in a range from 0.1 to 0.3 mm. Fatigue life results were given in the form of *S–N* curves and it was found that the adhesive thickness presented a limited influence on the fatigue life. Rushforth et al. [9] and Underhill and

* Corresponding author. Tel.: +351 244820300; fax: +351 244820310.
E-mail address: mpereira@estg.ipleiria.pt (A.M. Pereira).

0143-7496/$ - see front matter © 2009 Elsevier Ltd. All rights reserved.
doi:10.1016/j.ijadhadh.2009.02.009

Duquesnay [12] also investigated the life of epoxy-bonded single-lap shear joints, considering *S–N* curves. Hadavinia et al. [14,15] investigated the performance of adhesively bonded joints under monotonic and cyclic-fatigue loading, in 'dry' and 'wet' environments, employing different surface pre-treatments for the aluminium-alloy substrates. The joints were obtained with epoxy adhesive and aluminium-alloy substrates and investigated using a fracture-mechanics approach. Other authors [16–19] also applied fracture mechanics as the basis for their investigation of the fatigue behaviour of bonded joints. In another research work, Abel et al. [20] studied the cyclic-fatigue behaviour of organosilane-pretreated joints using a fracture mechanics approach. The cyclic-fatigue tests were conducted in 'dry' and 'wet' environments. The use of the γ-glycidoxypropyltrimethoxysilane pre-treatment provided an increased joint durability compared with a simple grit-blast and degrease treatment and, indeed, gave comparable results to using a chromic-acid etch pre-treatment. There are also many other fatigue studies of adhesive lap joints where the adherends are composite materials like those studied by Ferreira et al. [21].

This research work aims at understanding the fatigue behaviour of the single lap joints, extending the work previously reported by Pereira et al. [5] which investigated the static behaviour. Experimental work was carried out to understand the influence of adherends thickness and surface pre-treatment on fatigue strength. Complementary numerical work was also performed to study the influence of the adherends thickness on the adhesive's stress field, in order to explain the experimental trends.

2. Materials and experimental details

The material considered for the adherends was an aluminium alloy AA 6082-T6 in the form of thin sheets with a thickness of 1.0 and 1.5 mm. The adherends were bonded with a high strength epoxy adhesive of two components (Araldite 420 A/B from Huntsman, Cambridge, England). The adherends and the adhesive were characterized in terms of chemical composition and mechanical properties. Table 1 shows the chemical composition of the AA 6082-T6 sheets obtained from emission spectrometer analysis. Table 2 shows the mechanical properties of the aluminium alloy obtained from tension static tests and a resonant technique, while Fig. 1 presents the stress versus strain curves obtained with 1 mm thick specimens of aluminium alloy. Finally, Table 3 presents the mechanical properties of the adhesive obtained from Moura et al. [22]. The stress–strain curve of the Araldite 420 A/B adhesive was also obtained from Moura et al. [22].

The AA 6082-T6 sheets were cut in the dimension of $100 \times 25\,mm^2$ (Fig. 2) and their surfaces were cleaned with specified surface preparation before bonding, to eliminate surface contamination and promote adhesion. In previous work [5], the surface preparation was studied to maximize the static strength of adhesive joints. Five surface treatments were also studied, namely caustic etch (CE), Tucker's reagent (TR), sodium dichromate–sulphuric acid etch (CSA), abrasive polishing (AP) and solvent wiping (SW). The best shear strength was obtained for the CSA etch and AP. The process of preparing the surface using CSA etch was as follows: the specimens were immersed in a solution of sodium dichromate–sulphuric acid composed of 650 g H_2O (distilled), 75 g $Na_2Cr_2O_7$ and 275 g H_2SO_4 for 30 min, heated to 60–65 °C, rinsed under cold running water, then rinsed with

Table 2
Mechanical properties of aluminium alloy 6082-T6 adherend.

Tensile strength, σ_{UTS} (MPa)	305.6
Yield stress, σ_{ys} (MPa)	245.10
Elongation at failure, ε_r (%)	16.50
Young's modulus, E (GPa)	69.5
Shear modulus, G (GPa)	25.34
Poisson's ratio, ν (–)	0.346

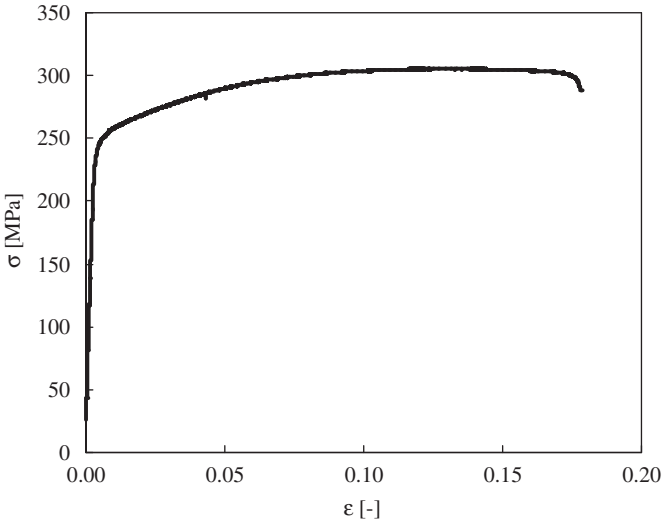

Fig. 1. Stress versus strain curve for the aluminium alloy (from 1 mm plates).

Table 3
Mechanical properties of the adhesive (Araldite 420 A/B) [22].

Tensile strength, σ_{UTS} (MPa)	30.29
Yield stress, σ_{ys} (MPa)	8.00
Young's modulus, E (GPa)	1.82
Poisson's ratio, ν (–)	0.3

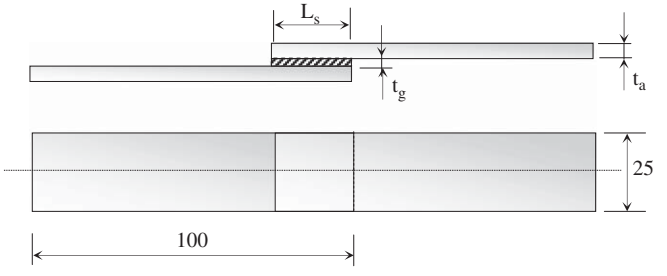

Fig. 2. Geometry of single lap joints (dimensions in mm).

Table 1
Chemical composition of aluminium alloy 6082-T6 adherend (wt%) ($AlSi_1MgMn$).

Element	Si	Fe	Cu	Mn	Mg	Zn	Ti	Cr	Al
Weight (%)	1.020	0.260	0.022	0.672	0.761	<0.005	0.0062	<0.002	97.240

deionized water and finally, at 65 °C, the surface was cleaned with dry air. The surface preparation technique with AP was as follows: the surface was mechanical abraded with silicon carbide paper P220 grade. At the end the surface was cleaned with dry air.

For adequate bonding, the specimens were compressed with a pressure of 0.157 MPa applied during all cure time (4 h at 50 °C). Experimental tests were performed using the lap-shear geometry represented in Fig. 2, having 20 mm of overlap length (L_s). The static shear strength was obtained using an electromechanical universal testing machine, Instron 4206. Tensile tests were performed up to the final failure of the joint, at a constant cross-head speed of 1 mm/min. Four specimens were tested for each test condition.

Three types of joints were submitted to fatigue testing: CSA surface preparation for 1.0 and 1.5 mm adherends thickness and AP surface preparation with 1.0 mm adherends thickness. The main objective was to understand the influence of the adherends thickness and surface preparation on the fatigue damage process.

The fatigue behaviour was studied using a servo-hydraulic mechanical testing machine, Dartec 100 kN. Tests were carried out at room temperature and constant amplitude with a load ratio ($R = P_{min}/P_{max}$) of 0.05, being P_{min} and P_{max} the minimum and maximum loads, respectively. A sinusoidal waveshape with a 20 Hz loading frequency was used. To minimize bending stresses during testing, both ends of the specimens were bonded to two plates of the same thickness. A total number of 33 fatigue tests were carried out. Fatigue results were plotted in the form of *S–N* curves and fatigue damage analysed in terms of stiffness decay against the number of cycles.

3. Experimental results

Table 4 summarizes the surface roughness and the static shear strength for different combinations of surface preparation and adherends thickness. Roughness measurements were carried out in two specimen directions (longitudinal and transversal) using a Mahr MarSurf Perthometer M2. The mean roughness depth (R_z) is the arithmetic mean value of the single roughness depths of five consecutive sampling lengths. The etch with sodium dichromate–sulphuric acid (CSA) produces an average roughness of 5.6 μm, while the abrasive polishing (AP) preparation gives the higher surface roughness of 7.2 μm. On the other hand, a limited influence of the surface treatment on the shear strength is observed. The increase of adherends thickness from 1 to 1.5 mm produced a significant increase of shear strength.

Similar shear strengths were obtained for both the surface preparation (CSA and AP) analysed in the case of the adherent thickness of 1.0 mm. This is because the loads in the static tests cause high plastic deformation in the aluminium promoting high strain in the adhesive. The yield stress of 6082-T6 aluminium alloy is presented in Table 2. Therefore, the failure of the joint is not justified by different surface preparation but by the aluminium yielding [23].

Table 4
Surface preparation details, shear strength and roughness.

Adherend thickness, t_a (mm)	Surface preparation	Average shear strength, τ_{UTS} (MPa)	Average roughness, R_z (μm)
1.0	CSA	15.64	5.6±0.73
1.5	CSA	22.69	5.6±0.73
1.0	AP	15.19	7.2±0.70

The failure surfaces show apparently a predominance of adhesive failure, although more accurate studies must be performed in order to check the possible formation of interphase adjacent to substrate. The best shear strengths, i.e., the most effective adhesions were obtained for the surface preparations that produced the lower surface roughness.

The *S–N* curves for the three types of joints are plotted in Fig. 3 in terms of the maximum nominal shear stress against the number of cycles to failure. The maximum fatigue strength was obtained for the CSA surface treatment. This treatment reaches a strength benefit of about 23% (for 10^5 cycles) compared with the abrasive polishing (AP). The increase of adherends thickness from 1 to 1.5 mm, tends to decrease fatigue strength by about 6% (for 10^5 cycles). Fig. 4 is a non-dimensional version of Fig. 3. The vertical axis shows a non-dimensional fatigue strength defined by the ratio between the maximum nominal shear stress and the ultimate tensile shear strength for each test series obtained in the static tests. The highest curve is again obtained for CSA technique. However, the lowest relative strength is now for the 1.5 mm adherends thickness, which means that the highest fatigue damage occurs for the highest adherends thickness. The abrasive polishing series showed fatigue damage between the two other series.

The load level in fatigue is relatively low compared with static testing, therefore the deformation of aluminium alloy

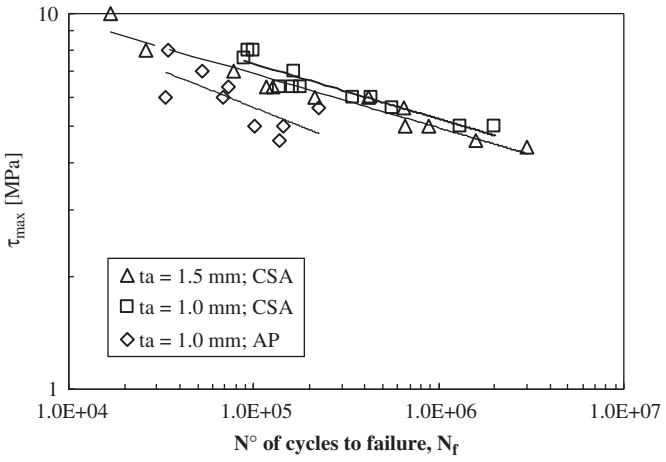

Fig. 3. Fatigue life curves of single-lap shear joints.

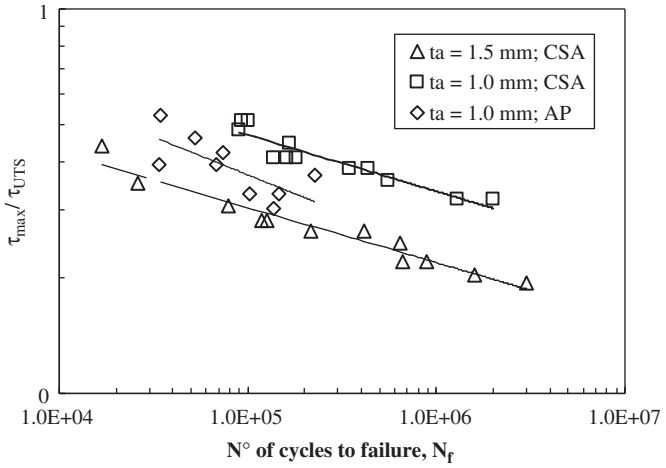

Fig. 4. Non-dimensional fatigue strength of single-lap shear joints.

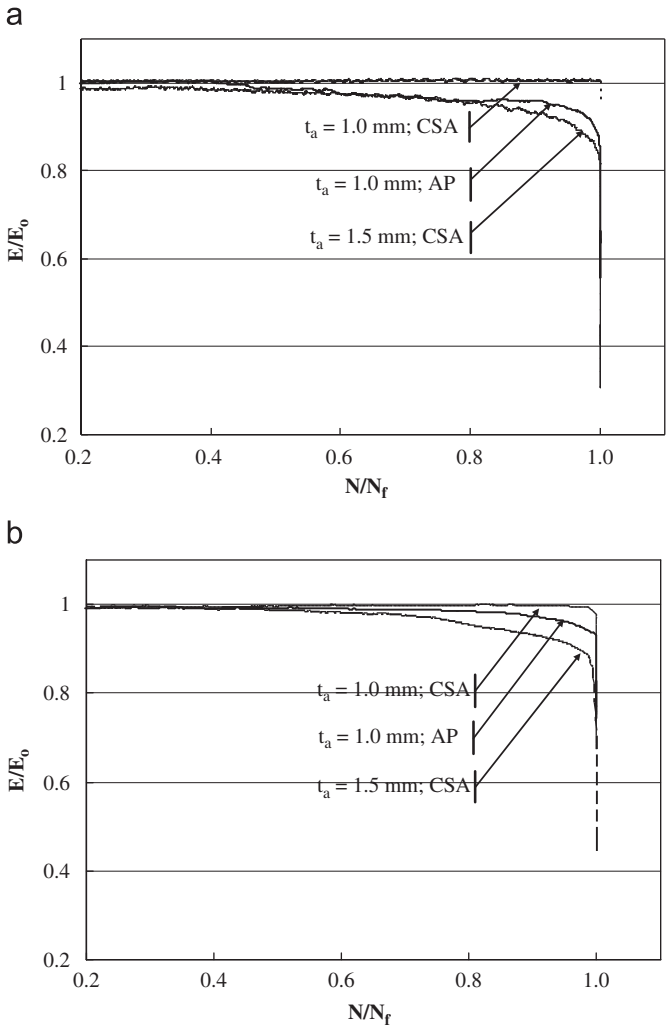

Fig. 5. Evolution of the global stiffness of single lap joints during fatigue testing for a maximum load of: (a) 2.5 kN and (b) 4.0 kN.

adherends was not observed experimentally. In spite, the aspect of failure surfaces is similar to that presented in Fig. 6 for static tests.

The different behaviour observed for each test series is expected to be related with failure mechanism changes. To confirm these changes, the stiffness decay along the fatigue process was analysed, the fracture surfaces were observed and a numerical study based on the finite element method was performed to obtain the stress field. Figs. 5(a) and (b) show the stiffness decay against the fatigue life for the three fatigue series and two maximum fatigue axial loads, 2.5 and 4 kN, respectively. The stiffness (E) is quantified by E/E_0, where E_0 is the initial value of E, and the fatigue life is expressed by N/N_f, being, N the current number of cycles and N_f the number of cycles to failure. During the fatigue tests, the peak load and displacement were monitored. E is the ratio $(P_{max}-P_{min})/(x_{max}-x_{min})$, where P_{max} and P_{min} are the maximum and minimum loads, respectively, and x_{max} and x_{min} are the maximum and minimum axial displacements, respectively. An early and/or high stiffness decreasing means high fatigue damage.

Results shown in Fig. 5 present for all cases a slight and stable decrease of E/E_0 until nearly final failure. Results in Fig. 5 confirm the conclusions obtained from Fig. 4, i.e., earlier and higher fatigue damage occurred for both the highest adherend thickness and the abrasive polishing process. The highest fatigue damage seems to be related with a high surface roughness and high stress perpendicular to adhesive surface (as shows σ_{yy} distribution in Fig. 10), which promotes more adhesive failure. Fig. 6 shows a typical failure surface of the single lap joint, for different adherends thickness and surface preparations techniques. An adhesive failure is evident, indicating that the interface is the weakest region of the joint. The same failure mode was observed in the three test series, but apparently the increase of adherends thickness and the use of abrasive polishing have increased the adhesive failure region, from direct observation of the specimens. The initiation of failures may be expected to occur at the corner points of bonded areas, which present higher stress and strain levels. The observed failure are in agreement with other studies [12,18,20].

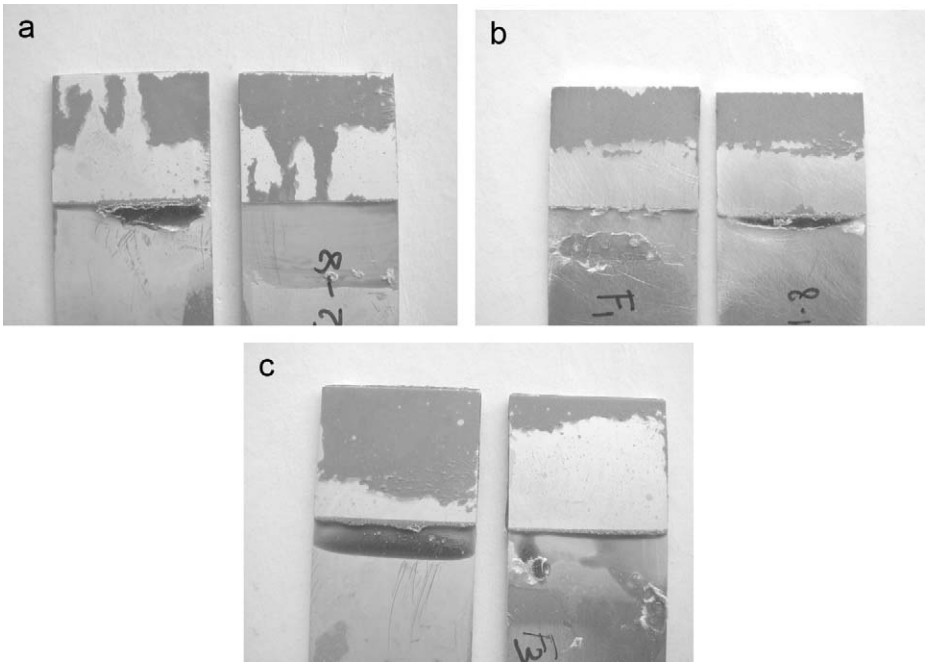

Fig. 6. Typical failure surface of the single lap joints tested in fatigue: (a) CSA surface preparation with 1.0 mm adherend thickness; (b) AP surface preparation with 1.0 mm adherend thickness; and (c) CSA surface preparation with 1.5 mm adherend thickness.

4. Numerical analysis

A numerical study was performed to study the influence of adherends thickness on the adhesive stress level. Fig. 7 shows the 2D physical model of the adhesive joint assumed to replicate the experimental test. Two values were considered for the adherends thickness ($t_a = 1$ and 1.5 mm), while the width (W) was maintained equal to 25 mm. One of the extremities of the specimen was fixed, while a uniform tension load was applied at the other. The rotation of the extremities was eliminated considering the boundary conditions represented, which simulated the rigidity of loading machine grips.

The aluminium alloy and the epoxy adhesive were assumed to be continuous, homogeneous, isotropic, elastic–plastic and obeying to the von Mises yield criterion and Prandtl–Reuss flow rule [24]. The elastic constants of the aluminium alloy presented in Table 2, obtained with a resonant technique, do not obey to $G = E/(2(1+\nu))$ (G is the shear modulus and ν is the Poisson's ratio). In fact, the aluminium alloy does not present a perfectly isotropic behaviour, however, for the numerical analysis, it was considered isotropic with $E = 69.5$ GPa and $\nu = 0.346$. The Voce model [25] was fitted to the experimental stress–strain curves of the adhesive as follows:

$$\sigma = C_0 + C_1 \cdot e^{C_2 \cdot \varepsilon^{C_3}} \quad (1)$$

with $C_0 = \sigma_{sat}$, $C_1 = -(\sigma_{sat} - \sigma_{ys})$, $C_2 = -149$, $C_3 = 0.8$, $\sigma_{sat} = 31$ MPa, being σ_{ys} the yield stress and σ_{sat} the asymptote of the curve. This model is in accordance with the experimental curves.

Fig. 8 shows the finite element discretization. Meshes were refined near the corner points, where greater variations of stress and strain are expected, as can be seen in Fig. 8b. Square elements were used to optimize the accuracy of the finite element method analysis. Elements' area near the corner points was $12.5 \times 12.5\ \mu m^2$, so eight elements were considered along the thickness of the adhesive, while the second layer of elements had sizes of 25 μm. Larger elements were considered at remote positions, in order to reduce the numerical effort.

Fig. 9 compares the numerical predictions with the experimental load–displacement curves. Displacements were obtained between two points, 50 mm distant each other, reproducing the extensometer distance. A good agreement exists between experimental results and plane stress numerical results. The yield stress of the 6082-T6 aluminium alloy is 245 MPa (Table 2) and the plates had a thickness of 1 mm and a width of 25 mm, so the plastic yield of aluminium alloy is expected to occur for loads of about 6125 N. The non-linearity of load–displacement curve in Fig. 9 can be mainly explained by the plastic deformation of the aluminium alloy.

Fig. 10 presents an out-of-plane stress (σ_{yy}) and a shear stress (τ_{xy}) at the mid-section of the adhesive. A symmetric distribution relatively to the centre of the overlap length ($L_s = 20$ mm) was

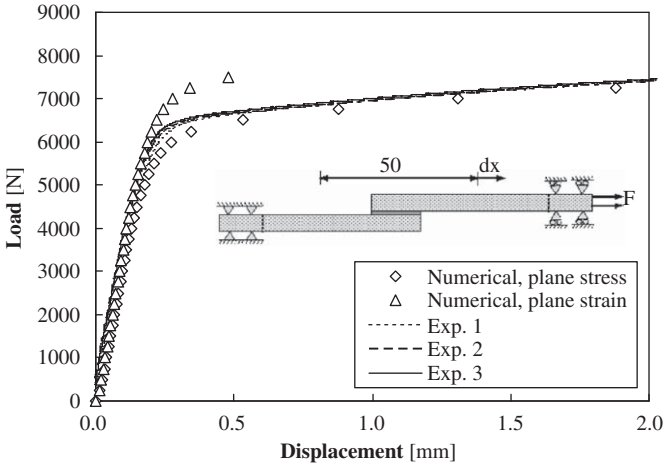

Fig. 9. Load versus displacement curves of single lap joint in static tension ($L_s = 20$ mm, $t_g = 0.1$ mm, $t_a = 1$ mm, full integration).

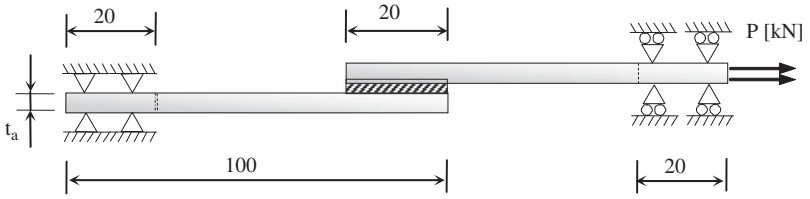

Fig. 7. Physical model of the single lap joint for the finite element analysis (dimensions in mm).

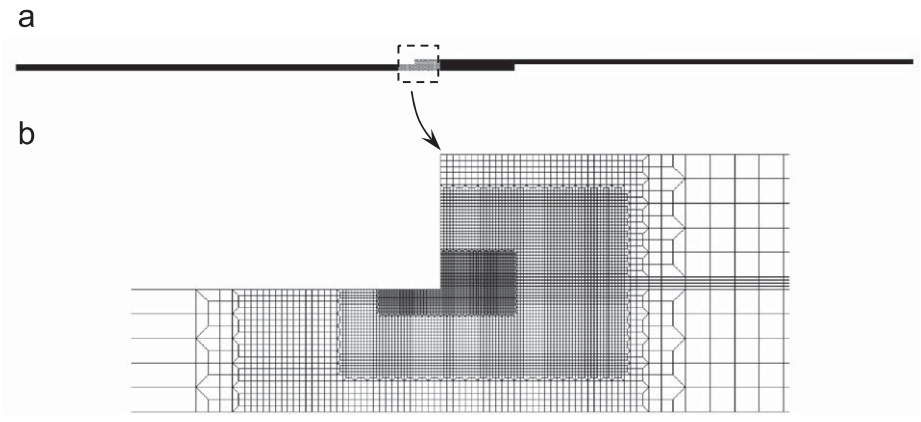

Fig. 8. (a) Shear lap joint specimen and (b) detail of finite element mesh (17 940 elements, 54 869 nodes).

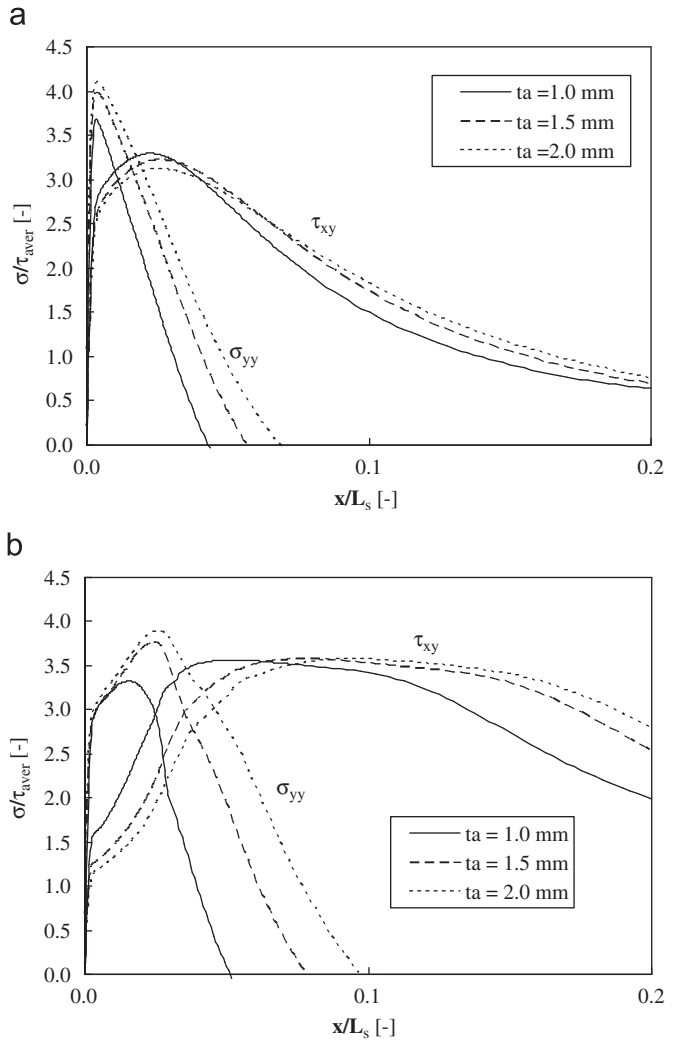

Fig. 10. Effect of specimen thickness on the stress distribution along the mid-section of the adhesive for plane stress state in a single lap joint: (a) $\tau_{aver} = 5$ MPa and (b) $\tau_{aver} = 10.2$ MPa ($L_s = 20$ mm; $t_g = 0.1$ mm).

obtained as expected. For plane stress conditions, the out-of-plane σ_{yy} presented peak values close to the corner point increasing with adherends thickness. The shear stress (τ_{xy}) has also a peak for relatively low loads, but for increasing forces a region with a constant value is formed, which is progressively extended with the load increase. The existence of this region with constant shear stress is related with the asymptotic behaviour of stress–strain curve of adhesive (Eq. (1)). The non-uniform distribution of stresses, with high localized stresses at the joint ends and very little stress in the central region is the main drawback of the lap-shear joint. Similar trends were obtained by Gonçalves et al. [26] and Pires et al. [7]. The rise of the load level increases the region with relatively large shear stress, which may influence the damage zone. Fig. 10 also shows the influence of adherends thickness (t_a) on the maximum values of the out-of-plane stress. The increase of t_a produces an increase of out-of-plane peak stresses, which seems to explain the variation of fatigue strength observed in Fig. 3.

5. Conclusions

The main conclusions obtained from this work are:

- The influence of the surface pre-treatment and its adherends thickness on the fatigue life of a aluminium alloy 6082-T6 adhesive joints were studied and correlated with the surface roughness, stress level and failure mechanisms.
- The maximum fatigue strength was obtained for the CSA surface treatment. This treatment reaches a strength benefit at about 23% (for 10^5 cycles) in comparison with an abrasive polishing. The increase of the adherends thickness from 1 to 1.5 mm tends to decrease the fatigue strength by about 6% (for 10^5 cycles).
- In all cases, a slight and stable decrease of E/E_0 until nearly final failure was observed during the tests. The earlier and higher fatigue damage was obtained for the highest adherend thickness (1.5 mm) and the abrasive polishing (AP) process. The highest fatigue damage was related with high surface roughness and high stress perpendicular to adhesive surface, facilitating adhesive failure.
- The numerical analysis showed the increase of the out-of-plane peak stresses with the increase of adherends thickness, which seems to explain the reduction of fatigue resistance observed.

References

[1] Chang B, Shi Y, Dong S. J Mater Process Technol 1999;87:230.
[2] Ghosh PK, Vivek. ISIJ Int 2003;43(1):85.
[3] Santos IO, Zang W, Gonçalves VM, Bay N, Martins PAF. Int J Mach Tools Manuf 2004;44:1431.
[4] Ferreira JAM, Silva H, Costa JD, Richardson M. Compos Part B Eng 2005;36:1.
[5] Pereira AM, Bártolo PJ, Ferreira JM, Antunes F. Virtual and rapid manufacturing: advanced research in virtual and rapid prototyping. London: Taylor and Francis; 2008. p. 597.
[6] de Morais AB, Pereira AB, Teixeira JP, Cavaleiro NC. Int J Adhes Adhes 2007;27:679.
[7] Pires I, Quintino L, Durodola JF, Beevers A. Int J Adhes Adhes 2003;23:215.
[8] da Silva LFM, Adams RD. Int J Adhes Adhes 2007;27:227.
[9] Rushforth MW, Bowen P, McAlpine E, Zhou X, Thompson GE. J Mater Process Technol 2004;153–154:359.
[10] Adams ANN, Kinloch AJ, Digby RP, Shaw SJ. Adhesion 99, Cambridge, September 15–17, 1999.
[11] Briskam P, Smith G. Int J Adhes Adhes 2000;20:33.
[12] Underhill PR, Duquesnay DL. Int J Adhes Adhes 2006;26:62.
[13] Krenk S, Jonsson J, Hansen LP. Eng Fract Mech 1996;53(6):859.
[14] Hadavinia H, Kinloch AJ, Little MSG, Taylor AC. Int J Adhes Adhes 2003; 23:449.
[15] Hadavinia H, Kinloch AJ, Little MSG, Taylor AC. Int J Adhes Adhes 2003; 23:463.
[16] Al-Ghamdi AH, Ashcroft IA, Crocombe AD, Abdel-Wahab MM. J Adhes 2003; 79:1161.
[17] Jethwa JK, Kinloch AJ. J Adhes 1997;61(1):71.
[18] Dickie RA, Haack LP, Jethwa JK, Kinloch AJ, Watts JF. J Adhes 1998;66:1.
[19] Curley AJ, Jethwa JK, Kinloch AJ, Taylor AC. J Adhes 1998;66:39.
[20] Abel M-L, Adams ANN, Kinloch AJ, Shaw SJ, Watts JF. Int J Adhes Adhes 2006; 26:50.
[21] Ferreira JAM, Reis PN, Costa JDM, Richardson MOW. Compos Sci Technol 2002;62:1373.
[22] de Moura MFSF, Daniaud R, Magalhães AG. Int J Adhes Adhes 2006;26:464.
[23] da Silva LFM, Critchlow GW, Figueiredo MAV. J Adhes Sci Technol 2008; 22:1477.
[24] Lemaitre J, Chaboche JL. Mechanics of solid materials. Cambridge: Cambridge University Press; 2000.
[25] Voce E. J Inst Met 1948;74:537.
[26] Gonçalves JPM, de Moura MFSF, de Castro PMST. Int J Adhes Adhes 2002; 22:357.